Adaptive PID Control of DC-link Voltage via DC/DC Buck-Boost Converter

Thanana Nuchkrua and Thananchai Leephakpreeda
Sirindhorn International Institute of Technology, Thammasat University, Pathum Thani 12121

Correspondence:
Thanana Nuchkrua
Sirindhorn International Institute of Technology, Thammasat University, Pathum Thani 12121
E-mail: Thanana.nuch@yahoo.com

Abstract

Mainly, a photovoltaic (PV) system is able to generate wide ranges of voltage and current at terminal output. However, a PV cell is required to functionally maintain a constant direct current (DC) voltage at a desired level during real-time variations of incident light illumination and ambient temperature. To obtain this goal, a power electronic convertor, that is a DC/DC converter together with control scheme topology, is implemented in this study. However, a conventional linear PID control law is not suitable to be an effective controller for regulating the output voltage of a DC/DC converter due to nonlinearity. An adaptive PID control scheme is proposed to stabilize the output voltage of the DC/DC converter, in order to maintain and stabilize the constant DC-link voltage in power line and load variations. The results of steady state and transient responses show that the performance of the proposed control scheme is more efficient than the conventional PID control scheme.

Keywords: DC/DC converter; PID Control; Buck-boost Converter; Photovoltaic system

1. Introduction

Recently, photovoltaic systems (PVs) increasingly play an important role in electrical energy. A PV module is a flat panel that uses photoelectric result to come up with electricity. PV energy system is one of the candidates for energy alternatives to solve the increasing environmental and energy problems. This implies that it will be used indefinitely to provide energy for usages such as homes, businesses, vehicles, and many other things. In order to get the maximum output power from the PV module, a power electronic system module is equipped with Maximum Power Point Tracking (MPPT), which operates the PV modules in a manner that allows the modules to produce maximum power. MPPT is a fully electronic system that varies the electrical operating point of the modules so that the modules are able to deliver maximum available power [1-2].

Generally, a DC/DC converter is also needed to take DC input from a PV module, and convert it back to a different DC voltage and current to exactly match the load system requirements. Some utility-interconnected PV systems operate at DC voltages in excess of 300 V before being inverted to standard alternating-current (AC). Whole systems are connected in parallel to the utility grid. Actually,

the electrical power generated by a DC/DC converter is important to be considered for electrical power quality, such as voltage fluctuation in transient response and constant voltage at steady state response. As a consequence, a control strategy for the DC/DC converter is important to achieve. It is designed to control the for accurate DC voltage in both transient and steady state characteristics, to provide suitable quality of electrical power.

Many previously published papers [3-10] presented lots of classical and modern control techniques, which showed the performances of their topologies on different load conditions. The models are not sufficient to represent systems with strong nonlinearity. Additionally, the performance of the controllers designed by frequency domain methods is dependent on the operating point, the parasitic elements of the system, and the load and line conditions. Good large signal stability can be achieved only by decreasing the bandwidth, resulting in slow dynamics. A state space model of buck-boost DC/DC converters suffers from the problem of Right-Half-Plane zero in its control to output a transfer function under continuous conduction mode (CCM). The movement of the zero on the S-plane as the operating point changes further compounds the problem.

Therefore, an adaptive controller is proposed to solve this problem. Combined use of fuzzy and logic, neural networks has been recognized as being promising [11]. In the past decades, Fuzzy Logic Control (FLC) has become a popular candidate for applications in power electronics when the process is too complex and nonlinear for analysis by conventional quantitative techniques [12,13]. However, the development of a fuzzy controller has to rely on the experience of the experts for determining the effective fuzzy rules.

Nowadays, there has been an increasing use of artificial neural networks (ANNs) for various applications, particularly because of their learning ability and adaptation using a nonlinear optimization algorithm, such as back-propagation. However, an undesired response, for example, high overshoot or a long settling time may occur during the learning period. To solve those drawbacks, neuro-fuzzy and conventional PID is introduced, an adaptive PID controller.

Generally, the basic concept of the Neural Control Method is first to use a structure-learning algorithm to find appropriate fuzzy logic rules and then use a parameter-learning algorithm to fine-tune the membership function and other parameters. The adapted PID gain is automatically tuned by a fuzzy rule. The initial gain of the PID algorithm is determined by Ziegler-Nichol technique. Actually, PID control can accelerate the output response to the desired error bound quickly. The proposed controller reveals that it is adaptive for all operating conditions. In this paper, the proposed control scheme can improve both transient and steady state responses of unstable power DC-link generated by a PV module through a DC/DC converter with constant load conditions, when compared with PI and PID control schemes. In addition, the simulation results from MATLAB/Simulink software are also presented.

The paper is organized as follows. In Section II, the mathematical modeling of a DC/DC converter is introduced. Section III demonstrates the system configuration. The proposed adaptive PID control scheme for control and stabilize DC-link is then expressed in Section IV. Simulation results from the control system are given in Section V. Finally, conclusions are drawn in Section VI.

2. Mathematical Modeling of a DC/DC Converter

The mathematical model of a boost type DC/DC converter in state space form is obtained by the application of basic laws governing the operation of the system. The schematic diagram of a DC/DC converter is shown in Fig. 1. The dynamic equations of this converter can be written as (5):

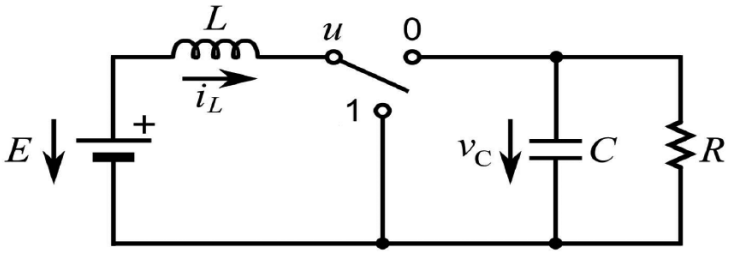

Fig. 1. Schematic diagram of a DC/DC converter.

$$\frac{di_L}{dt} = -(1-u)\frac{v_C}{L} + \frac{E}{L} \tag{1}$$

$$\frac{dv_C}{dt} = (1-u)\frac{i_L}{C} - \frac{v_C}{RC} \tag{2}$$

Where v_c and i_L are the output capacitor voltage and inductor current, respectively. The control input u is the switching function in the set of $\{0, 1\}$. Let 1- u be the mathematical function of an electronic switch. For the state equation, let $x_1 = i_L$ and $x_2 = v_C$, which yields:

$$\dot{x}_1 = -(1-u)\frac{1}{L}x_2 + \frac{E}{L} \tag{3}$$

$$\dot{x}_2 = (1-u)\frac{1}{C}x_1 - \frac{1}{RC}x_2 \tag{4}$$

The state space equation:

$$\begin{bmatrix} \dot{x}_1 \\ \dot{x}_2 \end{bmatrix} = \begin{bmatrix} 0 & -(1-u) \\ (1-u)\frac{1}{C} & -\frac{1}{RC} \end{bmatrix} \begin{bmatrix} x_1 \\ x_2 \end{bmatrix} + \begin{bmatrix} \frac{1}{L} \\ 0 \end{bmatrix} E \tag{5}$$

It is assumed that the boost converter is working in continuous conduction mode (CCM), in which the average value of the inductance current never drops to zero due to load variations [14].

3. System Configuration

Fig. 2 shows the DC/DC converter structure used to interface the PV array with the utility grid network through the power DC/AC inverter. The first stage is the DC/DC converter, which is directly connected to the inverter with MPPT for operating under the maximum power point profile. Without any voltage regulating capacitors of the DC/DC converter, the output voltage of PV array v_{pv} normally fluctuates in a wide range. To obtain a constant DC-link voltage at steady state, a robust controller is required in this application.

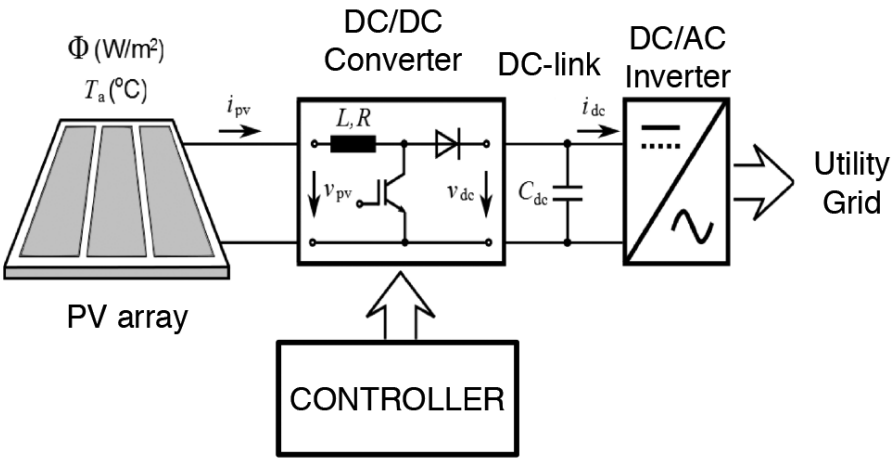

Fig. 2. The proposed diagram of system.

Normally, the MPPT gains maximum power available from a cell, at MPP, which only occurs at a single operating point in certain conditions. The power-voltage (PV) curves, at various levels of irradiance at 25ºC, are provided by a manufacturer, as shown in Fig. 4.

At the MPP of sunlight incident on a clear day (irradiance $\Phi = 1000\ W/m^2$), the output voltage of 17.1 V is obtained where losses are negligible. On the other hand, in shading conditions ($\Phi = 200\ W/m^2$) the output voltage is approximately 13.7 V. The gap of voltage between the maximum irradiance of 1000 and 200 W/m^2 is 3.6 V in the case of $\Phi = 200\ W/m^2$ at the MPP.

With data of PV and MPP, the conditions are set with an aim to control the output voltage of converter to be 320 V [15]. The voltage of the PV array (v_{pv}) is supplied to the DC/DC boost converter following the PV specification data, which is provided by the manufacturer. The selected polycrystalline PV array consists of 18 modules connected in series, and it can supply an output power of more than 1 *kW* from output voltage between 240 V and 300 V. The voltage of the PV cell varies with incident illumination and temperature, as depicted in Fig. 3.

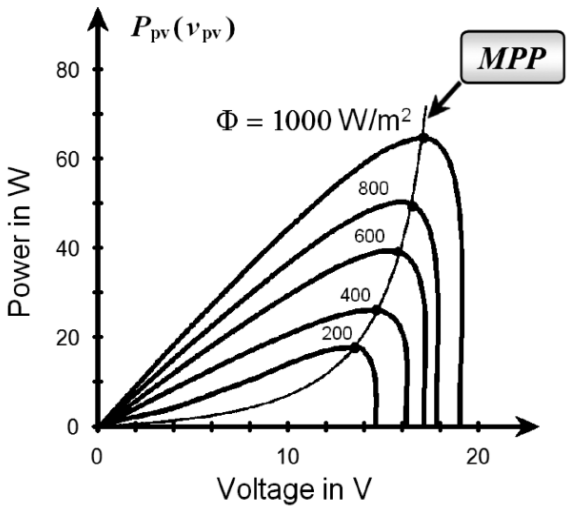

Fig. 3. Power-voltage curves at various levels of irradiance at 25ºC.

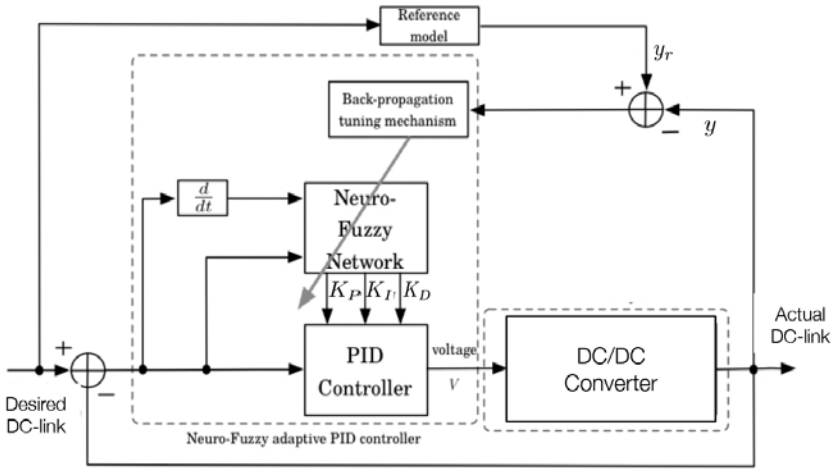

Fig. 4. The structure of Adaptive PID controller.

4. Control Scheme

The primary objective is to control the power generated by a PV array in order to satisfy the total instantaneous power demand in a highly disturbed environment.

Due to high nonlinearity of the parameter uncertainties of converter and environmental changes as described in the previous section, it is difficult to design the control algorithm for obtaining a robust controller with the linear conventional technique [16-19]. For this reason, it is suggested that a non-linear controller is required for that system. A neuro-fuzzy adaptive PID controller, as depicted in Fig. 4, is proposed to perform the switching signal for maintaining the stability of the DC-link at steady state, and improve transients. A neuro-fuzzy controller with fuzzy singleton rule is presented. In this paper, a triangle membership function is selected because of its simplicity. The triangle membership function equation is depicted in Fig. 5 and expressed as in (6)-(10).

For given e and $\dot{e}$, the parameters of the PID controller K_p, K_I, and K_D, are finely adapted in such a way that the difference between the reference model of DC-link and the actual DC-link, e, is minimized by applying a back-propagation tuning technique. In this paper, a first order model is selected as the reference model. This model has a unity DC gain resulting in no steady state error. The desired time constant (τ) is also selected, resulting in the following reference model as: $r = 1/(\tau s + 1)$.

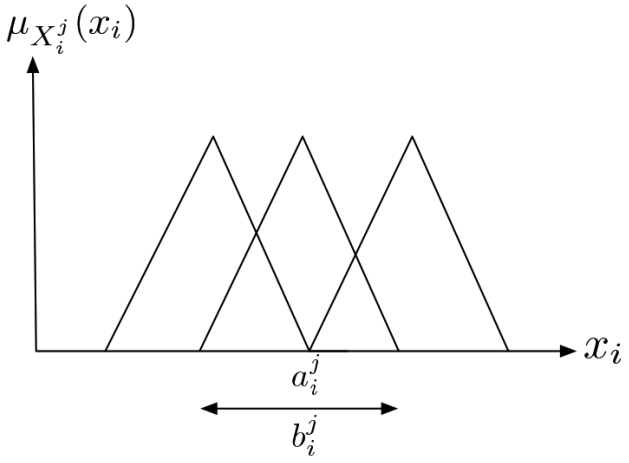

Fig. 5. Triangle member function.

$$\mu_{e_{A_i^j}}(e_i) = 1 - \frac{2\left|e_i - a_i^j\right|}{b_i^j}, \quad i = 1,2\ldots,n \quad j = 1,2\ldots,m, \tag{6}$$

$$\mu_{\dot{e}_{A_i^j}}(\dot{e}_i) = 1 - \frac{2\left|\dot{e}_i - a_i^j\right|}{b_i^j}, \quad i = 1,2\ldots,n \quad j = 1,2\ldots,m, \tag{7}$$

$$\mu_{P_{B_i^j}}(K_P) = 1 - \frac{2\left|K_P - a_i^j\right|}{b_i^j}, \quad i = 1,2\ldots,n \quad j = 1,2\ldots,m, \tag{8}$$

$$\mu_{I_{B_i^j}}(K_I) = 1 - \frac{2\left|K_I - a_i^j\right|}{b_i^j}, \quad i = 1,2\ldots,n \quad j = 1,2\ldots,m, \tag{9}$$

$$\mu_{D_{B_i^j}}(K_D) = 1 - \frac{2\left|K_D - a_i^j\right|}{b_i^j}, \quad i = 1,2\ldots,n \quad j = 1,2\ldots,m, \tag{10}$$

where x_i is the crisp set $x_i \in \{e_i, \dot{e}_i, K_P, K_I, K_D\}$ and $\mu_{X_i^j}(x_i)$ s the degree of membership function, $\mu_{X_i^j} \in \{\mu_{e_{A_i^j}}, \mu_{\dot{e}_{A_i^j}}, \mu_{P_{B_i^j}}, \mu_{I_{B_i^j}}, \mu_{D_{B_i^j}}\}$, m is the index of fuzzy rules, n is the index of membership function, e_i is the error value, $\dot{e}_i$ is the rate in error, a^i_j is the triangular center, b_i^j is the triangular width and the Fuzzy rule. The learning rule by the steepest descent technique is described as follows:

value, $\dot{e}_i$ is the rate in error, a_i^j is the triangular center, b_i^j

$$a_i^j(t+1) = a_i^j(t) - \eta_a \frac{\partial E}{\partial a_i^j}, \tag{11}$$

$$b_i^j(t+1) = b_i^j(t) - \eta_b \frac{\partial E}{\partial b_i^j}, \tag{12}$$

$$w_j(t+1) = w_j(t) - \eta_w \frac{\partial E}{\partial w_j}, \tag{13}$$

where

$$\frac{\partial E}{\partial a_i^j} = \frac{\mu_j(x)}{\sum_{j=1}^m \mu_j(x)}(y - y_r)(w_j - y)\,\mathrm{sgn}(x_i - a_i^j)\frac{2}{b_i^j \mu_{A_i^j}(x_i)}, \tag{14}$$

$$\frac{\partial E}{\partial b_i^j} = \frac{\mu_j(x)}{\sum_{j=1}^m \mu_j(x)}(y - y_r)(w_j - y)\frac{1}{b_i^j \mu_{A_i^j}(x_i)}(1 - \mu_{A_i^j}(x_i)), \tag{15}$$

$$\frac{\partial E}{\partial w_j} = \frac{\mu_j(x)}{\sum_{j=1}^m \mu_j(x)}(y - y_r), \tag{16}$$

In this work, to implement the inference mechanism, the fuzzy rules are defined as:

For K_P, in Table 1

Rule j: *if* e_i *is* ${}^{e}A_i^j$ *and* $\dot{e}_i$ *is* ${}^{\dot{e}}A_i^j$ *then* K_P *is* ${}^{P}B_i^j$

For K_I, in Table 2

Rule j: *if* e_i *is* ${}^{e}A_i^j$ *and* $\dot{e}_i$ *is* ${}^{\dot{e}}A_i^j$ *then* K_I *is* ${}^{I}B_i^j$

For K_D, in Table 3

Rule j: *if* e_i *is* ${}^{e}A_i^j$ *and* $\dot{e}_i$ *is* ${}^{\dot{e}}A_i^j$ *then* K_D *is* ${}^{D}B_i^j$

where ${}^{e}A$ and ${}^{\dot{e}}A$ are the input linguistic variables of the error and rate of change in error, respectively. ${}^{P}B$, ${}^{I}B$, *and* ${}^{D}B$ are the output linguistic variables of the adaptation of PID gain parameters. The adaptable gain parameters of PID, K_p, K_I, and K_D are determined by

$$K_P = \frac{\int_{K_P} \bigvee_{i=1}^{49} \left[\left(\mu_{e_{A_i^j}}(e) \wedge \mu_{\dot{e}_{A_i^j}}(\dot{e}) \right) \wedge \mu_{P_{B_i^j}}(K_P) \right] K_P d(K_P)}{\int_{K_P} \bigvee_{i=1}^{49} \left[\left(\mu_{e_{A_i^j}}(e) \wedge \mu_{\dot{e}_{A_i^j}}(\dot{e}) \right) \wedge \mu_{P_{B_i^j}}(K_P) \right] d(K_P)}, \tag{17}$$

$$K_I = \frac{\int_{K_I} \bigvee_{i=1}^{49} \left[\left(\mu_{e_{A_i^j}}(e) \wedge \mu_{\dot{e}_{A_i^j}}(\dot{e}) \right) \wedge \mu_{I_{B_i^j}}(K_I) \right] K_I d(K_I)}{\int_{K_I} \bigvee_{i=1}^{49} \left[\left(\mu_{e_{A_i^j}}(e) \wedge \mu_{\dot{e}_{A_i^j}}(\dot{e}) \right) \wedge \mu_{I_{B_i^j}}(K_I) \right] d(K_I)}, \tag{18}$$

$$K_D = \frac{\int_{K_D} \bigvee_{i=1}^{49} \left[\left(\mu_{e_{A_i^j}}(e) \wedge \mu_{\dot{e}_{A_i^j}}(\dot{e}) \right) \wedge \mu_{D_{B_i^j}}(K_D) \right] K_D d(K_D)}{\int_{K_D} \bigvee_{i=1}^{49} \left[\left(\mu_{e_{A_i^j}}(e) \wedge \mu_{\dot{e}_{A_i^j}}(\dot{e}) \right) \wedge \mu_{D_{B_i^j}}(K_D) \right] d(K_D)}, \tag{19}$$

Table 1. Fuzzy rules for K_p.

e \ $\dot{e}$	NB	NM	NS	ZE	PS	PM	PB
NB	PB	PB	PM	PM	PS	ZE	ZE
NM	PB	PB	PM	PS	PS	ZE	NS
NS	PM	PM	PM	PS	ZE	NS	NS
ZE	PM	PM	PS	ZE	NS	NM	NM
PS	PS	PS	ZE	NS	NS	NM	NM
PM	PS	ZE	NS	NM	NM	NM	NB
PB	ZE	ZE	NM	NM	NM	NB	NB

Table 2. Fuzzy rules for K_I.

e \ $\dot{e}$	NB	NM	NS	ZE	PS	PM	PB
NB	NB	NB	NM	NM	NS	ZE	ZE
NM	NB	NB	NM	NS	NS	ZE	ZE
NS	NB	NM	NS	NS	ZE	PS	PS
ZE	NM	NM	NS	ZE	PS	PM	PM
PS	NM	NS	ZE	PS	PS	PM	PB
PM	ZE	ZE	PS	PS	PM	PB	PB
PB	ZE	ZE	PS	PM	PM	PB	PB

Table 3. Fuzzy rules for K_D.

e \ $\dot{e}$	NB	NM	NS	ZE	PS	PM	PB
NB	PS	NS	NB	NB	NB	NM	PS
NM	PS	NS	NB	NM	NM	NS	ZE
NS	ZE	NS	NM	NM	NS	NS	ZE
ZE	ZE	NS	NS	NS	NS	NS	ZE
PS	ZE	ZE	ZE	ZE	ZE	ZE	ZE
PM	PB	NS	PS	PS	PS	PS	PB
PB	PB	PM	PM	PM	PS	PS	PB

Fig. 6 shows the adjustments of the PID gains for the neuro-fuzzy modules. As expected, it can be observed from the curved surfaces that the functions of the PID-gain adjustments are non-linear with respect to input variables of the error and the rate of change in error.

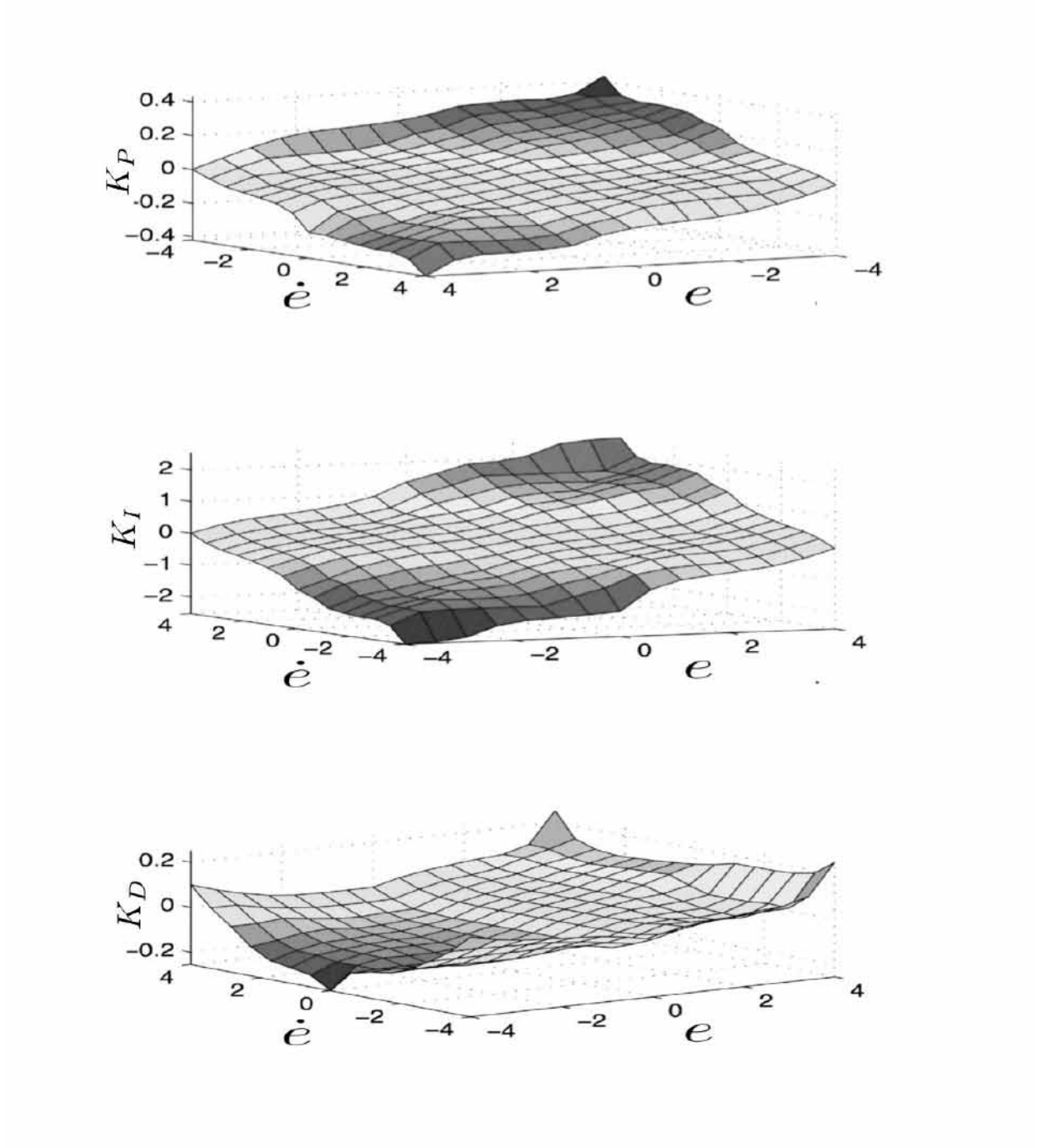

Fig. 6. The adjustments of PID gains for adaptive PID control.

5. Result And Discussion

To evaluate performances of the proposed system, computer simulations are conducted using MATLAB/SIMULINK® programming for simulating under various conditions. The PV parameters and configuration structure are described in the previous section with parameters of boost DC/DC converter given in Table I. In the proposed method, the estimated gains of the PID controller are recommended by the Ziegler-Nichols tuning rule where they are related to the unit-step-response characteristics of the controlled system.

Fig. 7 is the simulation results selected to demonstrate the more significant aspects of the system behaviors under the standard climatic conditions (1000 W/m^2 and 25 ºC). Figures 7(b), 7(c), and 7(d) show the DC-link regulated voltages of 320 V when the PV power source operates following its characteristics as shown in Figure 7(a). The transient responses and steady state errors on DC-link stabilized by the various control schemes are presented in Fig. 7(b), 7(c), and 7(d).

In Fig. 7(b) and 7(c), DC-link voltage is respectively controlled by PI and PID in order to maintain the constant voltage of 320 V (the red line). In transient response, PI can improve the rise time but it has an error in steady state response when PV power source voltage decreases from 300 V to 60 V as shown in Fig. 7(a). In Fig. 7(d), it is seen that the proposed controller can improve those drawbacks of PI and PID in both transient and steady state responses. An overshoot of DC-link voltage can be decreased lower than PI and PID, approximately 80 V, when operating with adaptive PID. In addition, adaptive PID is robust against climatic environmental disturbances for maintaining DC-link voltage at a steady state of 320 V, as depicted in Fig. 7(d).

Table 1. Parameters of the Boost DC/DC Converter.

Variables	Definition
Inductor (L)	1.5 mH
Capacitor (C)	20 μF
Switching frequency ($1/T$)	10 kHz

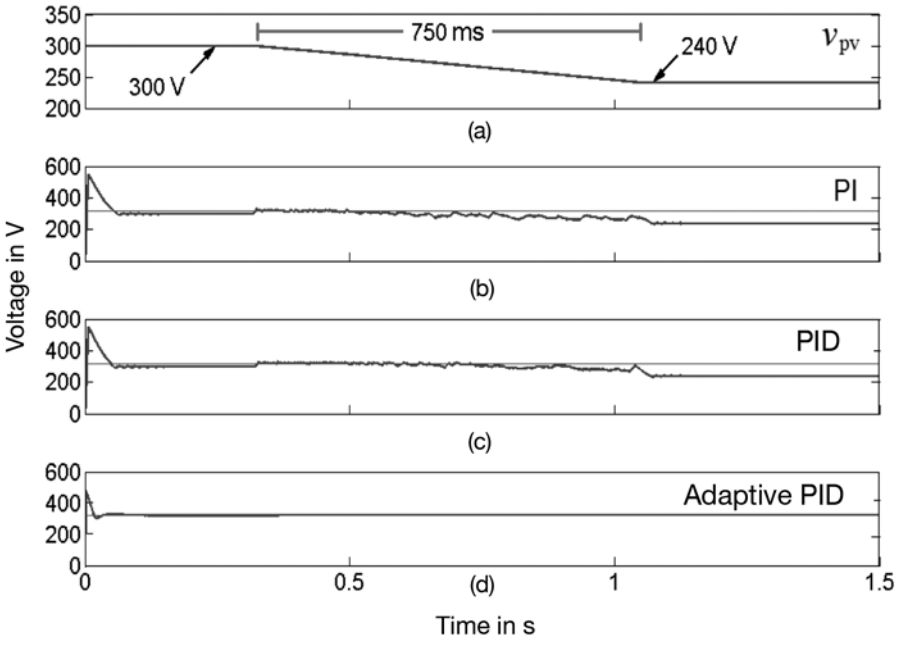

Fig. 7. The simulation results of line variation.

The simulation results of load variation are shown in Fig. 8. When the converter output power changes from 1 *k*W to 2 *k*W, at about 50-V, oscillating voltage occurs on the DC-link of the PI control scheme and a 30 V oscillating voltage on the DC-link of the PID control scheme (Figs. 8(b) and 8(c)). In contrast, the DC-link voltage, controlled by adaptive PID control scheme (Fig. 8(d)), is nearly smooth. The proposed controller improves the transient response and also reduces steady state error of the DC-link voltage.

6. Conclusion

The control strategies of the PV power supply system are compared in this paper. The proposed models are implemented in MATLAB/Simulink software. This paper also describes the dynamic behavior of PV under standard climate conditions using the operation of MPPT. The simulation results are obtained for a normal regime. In this paper, adaptive PID is compared with PI and PID control. From the simulation results, PI and PID control strategies do not control against one of non-linear controls used to stabilize DC-link to the variations of the PV power source. Steady state error from PI and PID control is significant. This means the classical control strategies should have some limitations for controlling. As a result of this fact, the proposed technique, adaptive PID, is suitable for the variable structure nature of the DC/DC converter and variations due to the nature of irradiation of the sun that could not be predicted. Adaptive PID can not only improve the transient response, but also reduces the steady state error of the DC-link voltage.

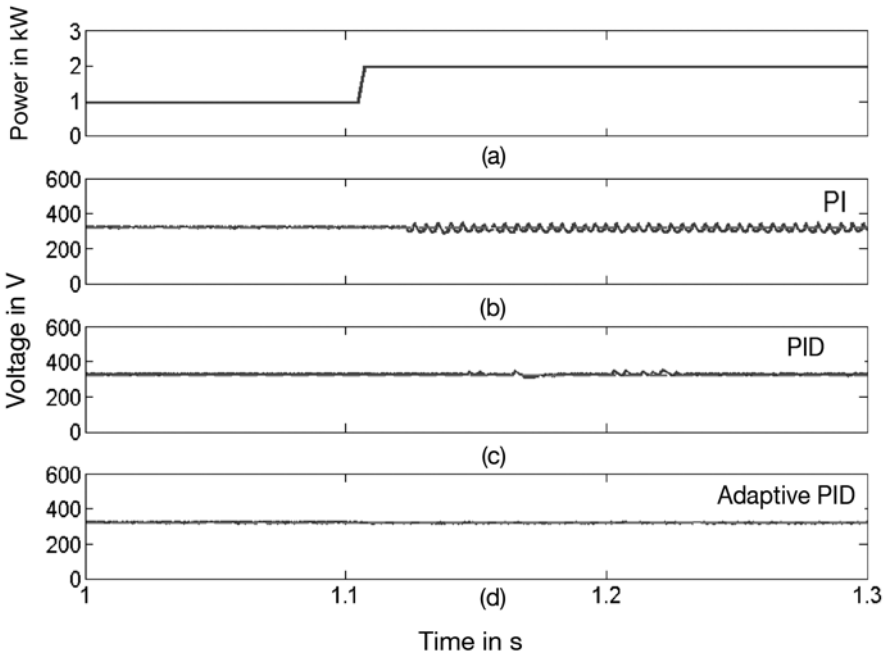

Fig. 8. The simulation results of load variation.

7. References

[1] Femia, N., Petrone, G., Spagnuolo, G., and Vitelli, M., Optimization of perturb and observe maximum power point tracking method, IEEE Trans. on Power Electronics, Vol. 20, pp. 963-973, July, 2005.

[2] Koutroulis, E., Kalaitzakis, K., and Voulgaris, N.C., Development of a microcontroller-based, photovoltaic maximum power point tracking control system, IEEE Trans. on Power Electronics, Vol. 16, pp. 46-54, January, 2001.

[3] Raviraj, V. S. C. and Sen, P. C. , A Comparative study of proportional-Integral, sliding mode, and fuzzy logic controllers for power converters, IEEE Trans. Ind. Appl., Vol. 33, No. 2, pp. 401-411, Mar-Apr, 1997.

[4] López, M. , de Vicuña, L. G., Astilla, M. C, Gayà, P., and López, O., Current distribution control design for paralleled DC/DC converters using sliding-mode control, IEEE Trans. Ind. Electron., Vol. 51, No. 2, pp. 419-428, Apr, 2004.

[5] Sanchis, P., Ursæa, A., Gubía, E., and Marroyo, L., Boost DC-AC inverter: A new control strategy, IEEE Trans. Power. Electron., Vol. 20, No. 2, pp. 343-353, Mar, 2005.

[6] Tan, S. C. , Lai, Y. M., Tse, C. K. , Martínez-Salamero, L., and Wu, C.K., A fast-response sliding-mode controller for boost-type converters with a wide range of operating conditions, IEEE Trans. Ind. Electron., Vol. 54, No. 6, pp. 3276-3286, Dec. 2007.

[7] Agorreta, J.L., Reinaldos, L., González, R., Borrega, M., Balda, J., and Marroyo, L., Switching technique applied to PWM boost converter operating in mixed conduction mode for PV systems, IEEE Trans. Ind. Electron., Vol. 56, No. 11, pp. 4363-4373, Nov. 2009.

[8] Khiari, B., Sellami, A., Andoulsi, R., M'Hiri, R., Ksouri, M., Discrete control by sliding mode of a photovoltaic System, in Proc. 1st Int. Symp. Control, Communications and Signal Processing, pp. 469-474, 2004.

[9] Diallo, D., Belkacem, F., Berthelot, E., Design and control of a low power DC-DC converter fed by a photovoltaic array, in Proc. Int. Electric Machines & Drives Conf. (IEMDC'07), Vol. 2, pp. 1298-1293, May 3-5, 2007.

[10] Plaza, D., De Keyser, R., and Bonilla, J., Model predictiveand sliding mode control of a boost converter, in Proc. Int. Symp. SPEEDAM 2008, June 11-13, 2008, pp. 37-42, 2008.

[11] Chen M, Linkens DA. A hybrid neuro-fuzzy PID controller, Fuzzy Sets Syst., Vol. 99, No. 11, pp. 27-36.

[12] Mattavelli, P., Uso, S., Spiazzi, G., and Tenti, P., A Fuzzy control of power factor preregulators, in IEEE-ISA'95 Conf., Vol. 3, pp. 2678-2685, 1993.

[13] Gupta, T., Boudreaux, R.R., Nelm, R.M., and Hung, J.Y., Implementation of fuzzy controller for DC/DC converters using an inexpensive 8-b microcontroller, IEEE Transactions Industrial Electronics, Vol. 44, pp. 661-669, 1997.

[14] Dylan, D., David, C., and Yim-Shu, L., A single-switch continuous-conductiob-mode boost converter with reduced recovery and switching losses, IEEE Transaction on industrial electronics, Vol. 50, No. 4, pp. 37-42, August, 2003.

[15] IEC 1727, Characteristics of the utility interface for photovoltaic (PV) systems, 2002.

[16] Tse, C. K., and Lai, Y. M., Control of bifurcation in current-programmed DC/DC converters: a reexamination of slope compensation, Proc. of IEEE International Symposium on Circuits and Systems, pp. I-671–674, June 2000.

[17] Lei Hong; Hui Yan; Yunfeng Xi; Xiao Chen; Guozhu Chen, Design of DC-bus voltage controller for Hybrid Active Power Filter based on pole-zero placement, Industrial Electronics (ISIE), 2011 IEEE International Symposium on, pp. 211-216.

[18] Huang Xinming; Liu Jinjun; Zhang Hui A Unified Compensator Design Based on Instantaneous Energy Equilibrium Model for the DC Link Voltage Control of UPQC, Applied Power Electronics Conference and Exposition, APEC, Twenty-Fourth Annual IEEE, pp. 1577-1582, 2009.

[19] Tan Zhili; Zhu Dongjiao Design of dc Voltage Controller for UPQC by Using its Small Signal Model, Electrical and Control Engineering (ICECE), 2010 International Conference on, pp. 3572-3575.